SUPPLEMENTAL FIGURES

Small molecule–based inhibition of MEK1/2 proteins dampens inflammatory responses to malaria, reduces parasite load, and mitigates pathogenic outcomes*

Xianzhu Wu[‡], Kiran K. Dayanand[‡], Ramesh P. Thylur[‡], Christopher C. Norbury[§], and D. Channe Gowda[‡,1]

From the [‡]Department of Biochemistry and Molecular Biology, Pennsylvania State University College of Medicine, Hershey, PA 17033 and the [§]Department of Microbiology and Immunology, Pennsylvania State University College of Medicine, Hershey, PA 17033

Running title: Targeting MEK1/2 Prevents Malaria Pathogenesis

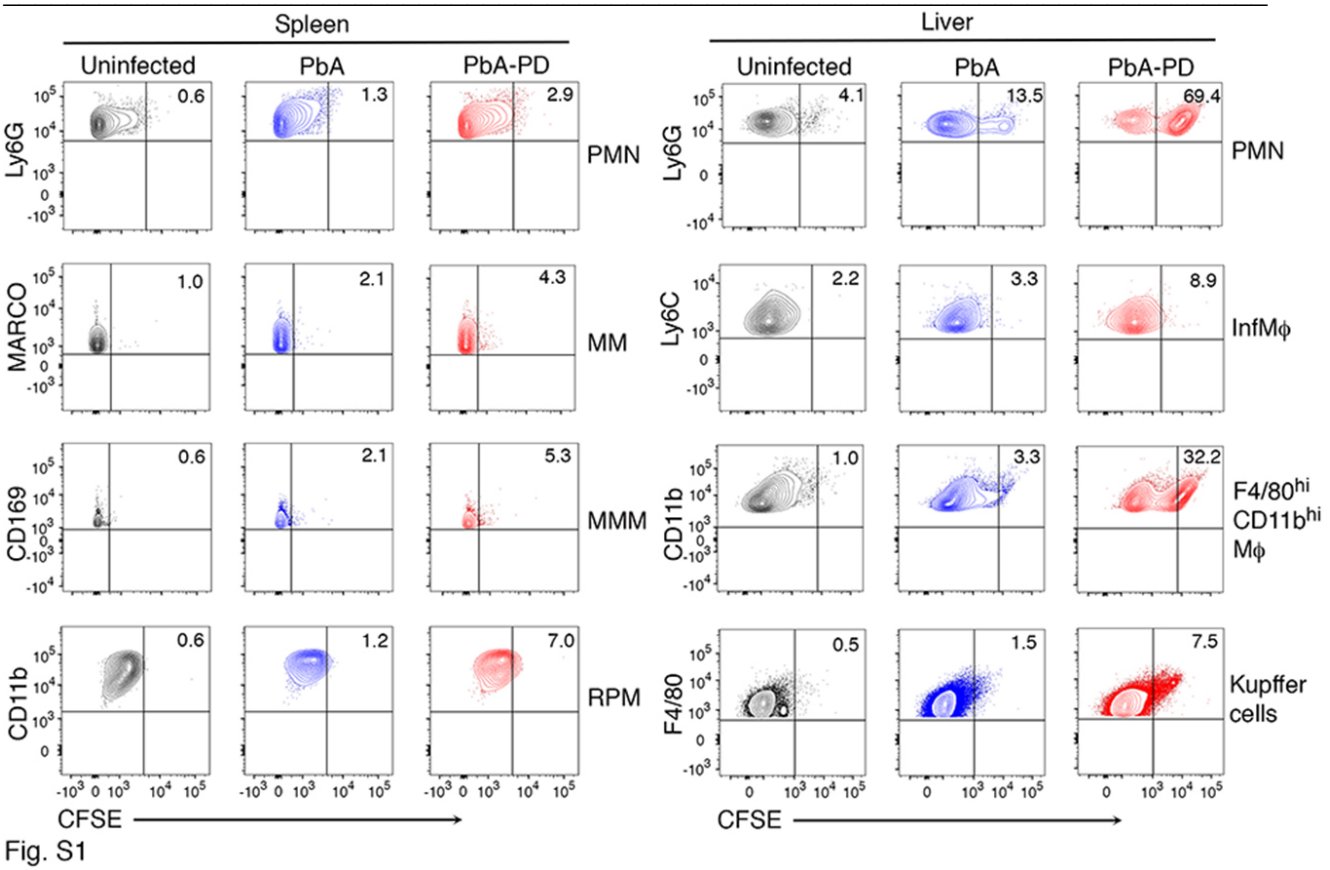

Fig. S1

FIGURE S1. **Analysis of the effect of inhibiting MEK1/2 signaling on the phagocytic uptake of malaria parasite-infected red blood cells in PbA-infected mice.** Shown is the analysis of spleen and liver neutrophils (peripheral mononuclear cells, PMNs) and macrophages (Mϕs) that phagocytosed CFSE-labeled IRBCs in vehicle-treated (PbA) and PD-treated (PbA-PD) mice (results are given in Fig. 4). The strategies for gating spleen and liver cells are shown in Fig. 4*A* and Fig. 4*C*, respectively. Cells from uninfected mice, which were not administered with CFSE-labeled IRBCs, were analyzed as controls. The extent of phagocytic uptake of IRBCs by spleen and liver PMNs and Mϕ subsets are shown in Fig. 4, *B* and *D*. MM, marginal zone Mϕs; MMM, marginal zone metallophilic Mϕs; RPM, red pulp Mϕs: InfMϕ, inflammatory macrophages.

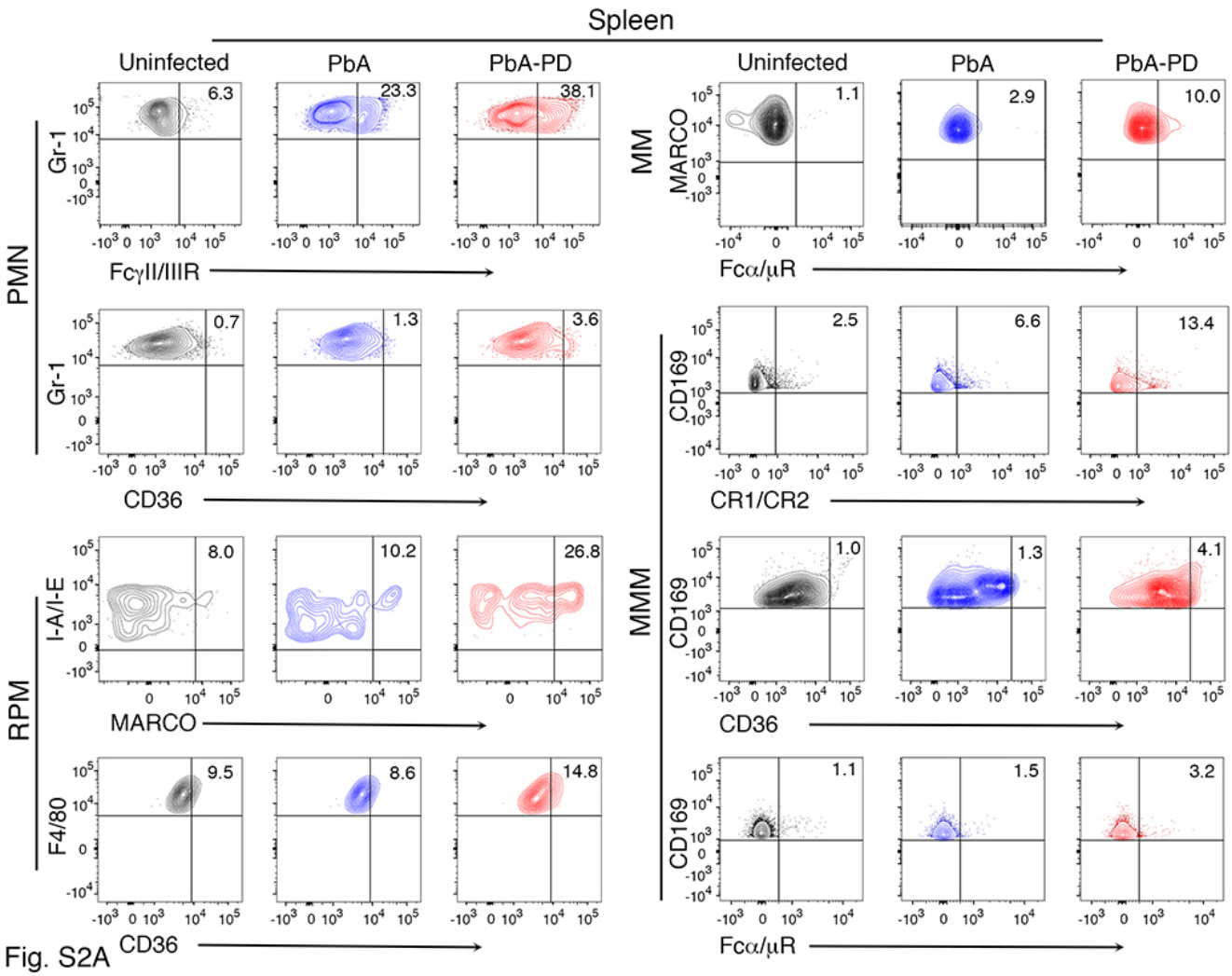
Spleen
Uninfected
PbA
PbA-PD
PMN
Gr-1
FcγII/IIIR
6.3
23.3
38.1
Gr-1
CD36
0.7
1.3
3.6
RPM
I-A/I-E
MARCO
8.0
10.2
26.8
F4/80
CD36
9.5
8.6
14.8
MM
MARCO
Fcα/μR
1.1
2.9
10.0
CD169
CR1/CR2
2.5
6.6
13.4
MMM
CD169
CD36
1.0
1.3
4.1
CD169
Fcα/μR
1.1
1.5
3.2

Fig. S2A

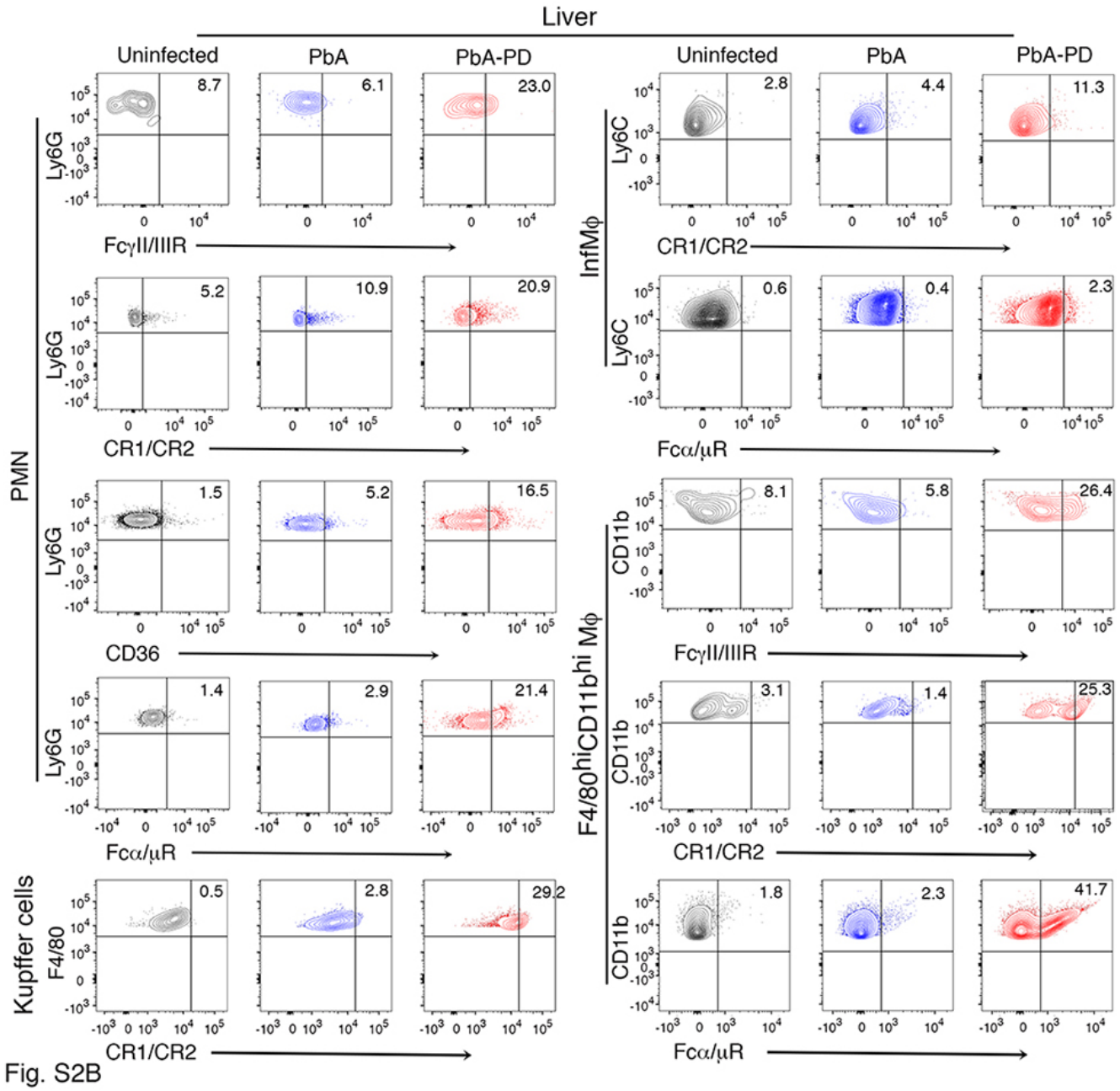

Fig. S2B

FIGURE S2. **Analysis of the effect of targeting MEK1/2 signaling inhibition on the expression of phagocytic receptors in PbA-infected mice.** At 5-day pi, the spleen and liver cells were stained with antibodies against phagocytic receptors and markers proteins, and analyzed by flow cytometry. The gating strategies for analyzing the cells are shown in Fig. 4*A* and Fig. 4*C*. Cells from uninfected mice were analyzed as controls. MM, marginal zone Mϕs; MMM, marginal zone metallophilic Mϕs; RPM, red pulp Mϕs: InfMϕ, inflammatory macrophages. Shown are the analysis of phagocytic receptor expression by spleen (Fig. S2*A*) and liver (Fig. S2*B*) neutrophils (PMNs) and macrophages (Mϕs) in control and PD-treated PbA-infected mice. The data are presented in Fig. 4, *E* and *F*.

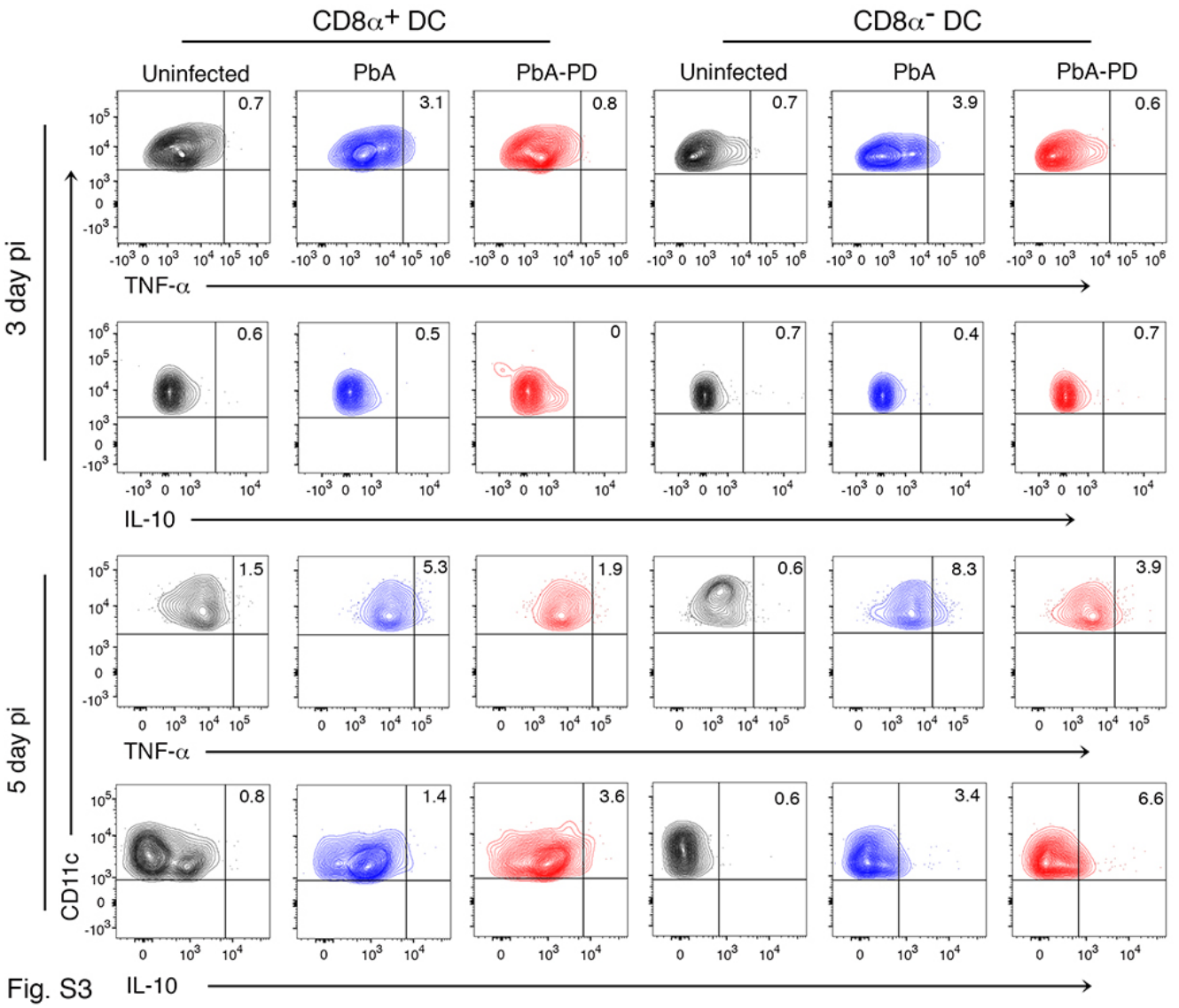

Fig. S3

FIGURE S3. **Analysis of the effect of targeting MEK1/2 on malaria-induced cytokine responses by spleen DCs.** Cytokine-producing DCs in vehicle-treated and PD-treated PbA-infected mice were analyzed. Spleen cells from mice at 3-day and 5-day pi were stained for surface marker proteins and intracellular cytokines, and analyzed by flow cytometry. The gating strategy of $CD11c^{hi}MHCII^{hi}CD8\alpha^{+}$ and $CD11c^{hi}MHCII^{hi}CD8\alpha^{-}$ DC subsets is shown in Fig 6*B*. The results are shown in Fig. 6, *C* and *D*.

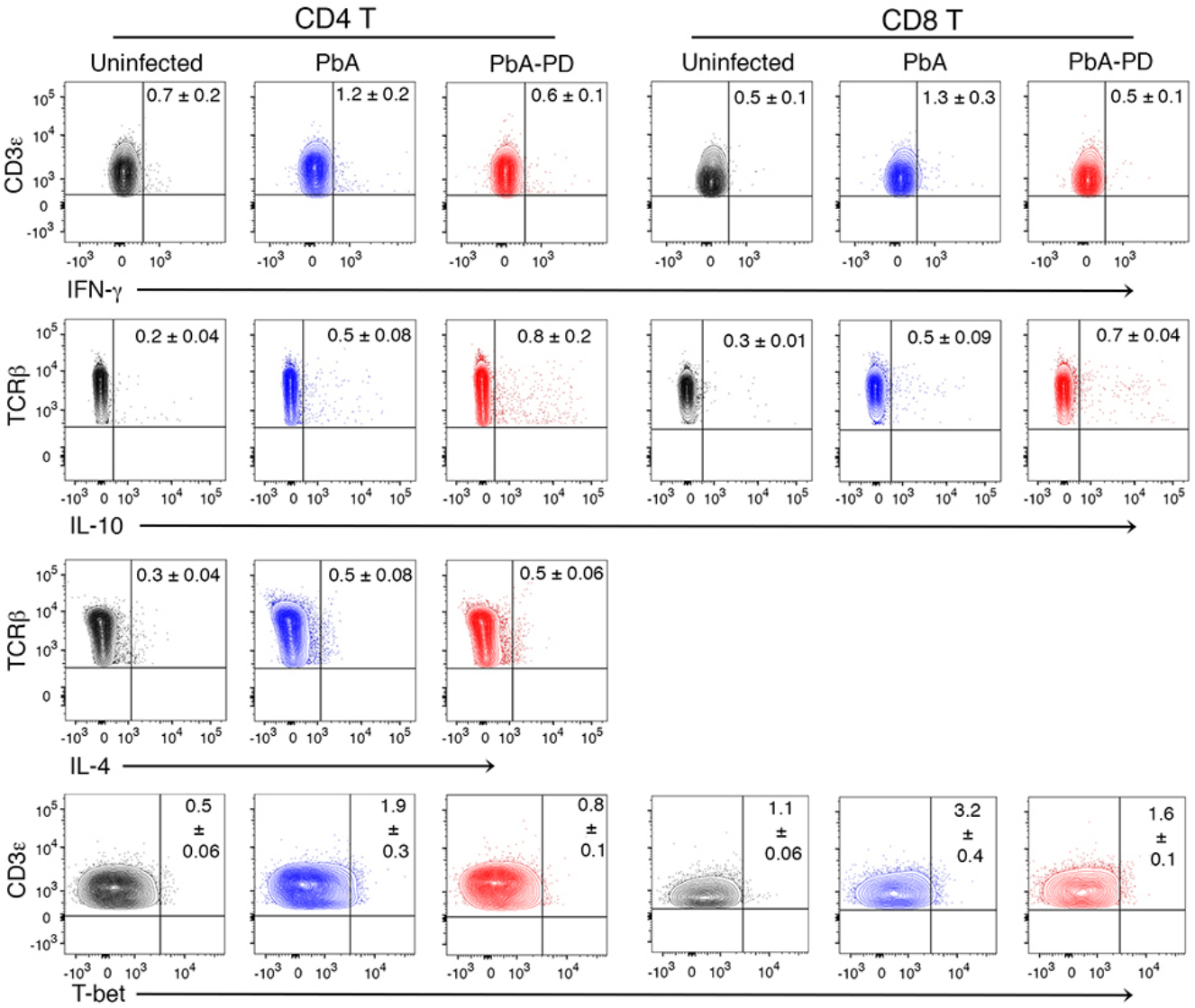
CD4 T
CD8 T
Uninfected
PbA
PbA-PD
Uninfected
PbA
PbA-PD
CD3ε
0.7 ± 0.2
1.2 ± 0.2
0.6 ± 0.1
0.5 ± 0.1
1.3 ± 0.3
0.5 ± 0.1
IFN-γ
TCRβ
0.2 ± 0.04
0.5 ± 0.08
0.8 ± 0.2
0.3 ± 0.01
0.5 ± 0.09
0.7 ± 0.04
IL-10
TCRβ
0.3 ± 0.04
0.5 ± 0.08
0.5 ± 0.06
IL-4
CD3ε
0.5 ± 0.06
1.9 ± 0.3
0.8 ± 0.1
1.1 ± 0.06
3.2 ± 0.4
1.6 ± 0.1
T-bet

Fig. S4A

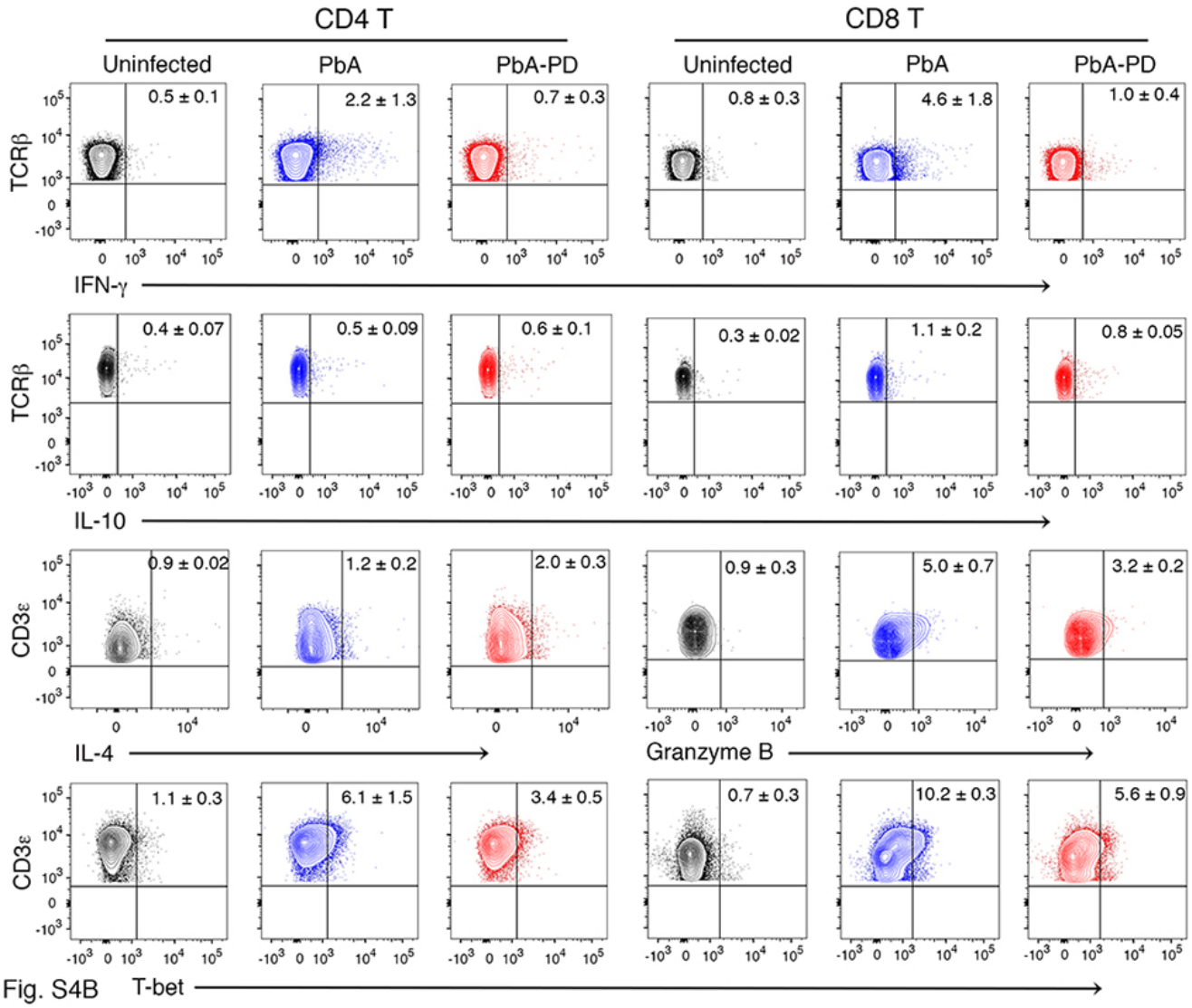

FIGURE S4. **Analysis of the effect of ERK1/2 signaling inhibition on T cell responses in PbA-infected mice**. Spleens cells from control and PD-treated mice at 4-day (Fig S4*A*) and 6-day (Fig S4*B*) pi were stained with antibodies against surface markers, fixed, stained with the antibodies against indicated proteins, and analyzed by flow cytometery. Spleen cells from uninfected mice were analyzed as controls. Shown are the analysis of cytokine-, T-bet-, and granzyme B-expression by CD4 and CD8 T cells. The gating strategy of CD4 and CD8 T cells and the results are shown in Fig. 9*A-C*.

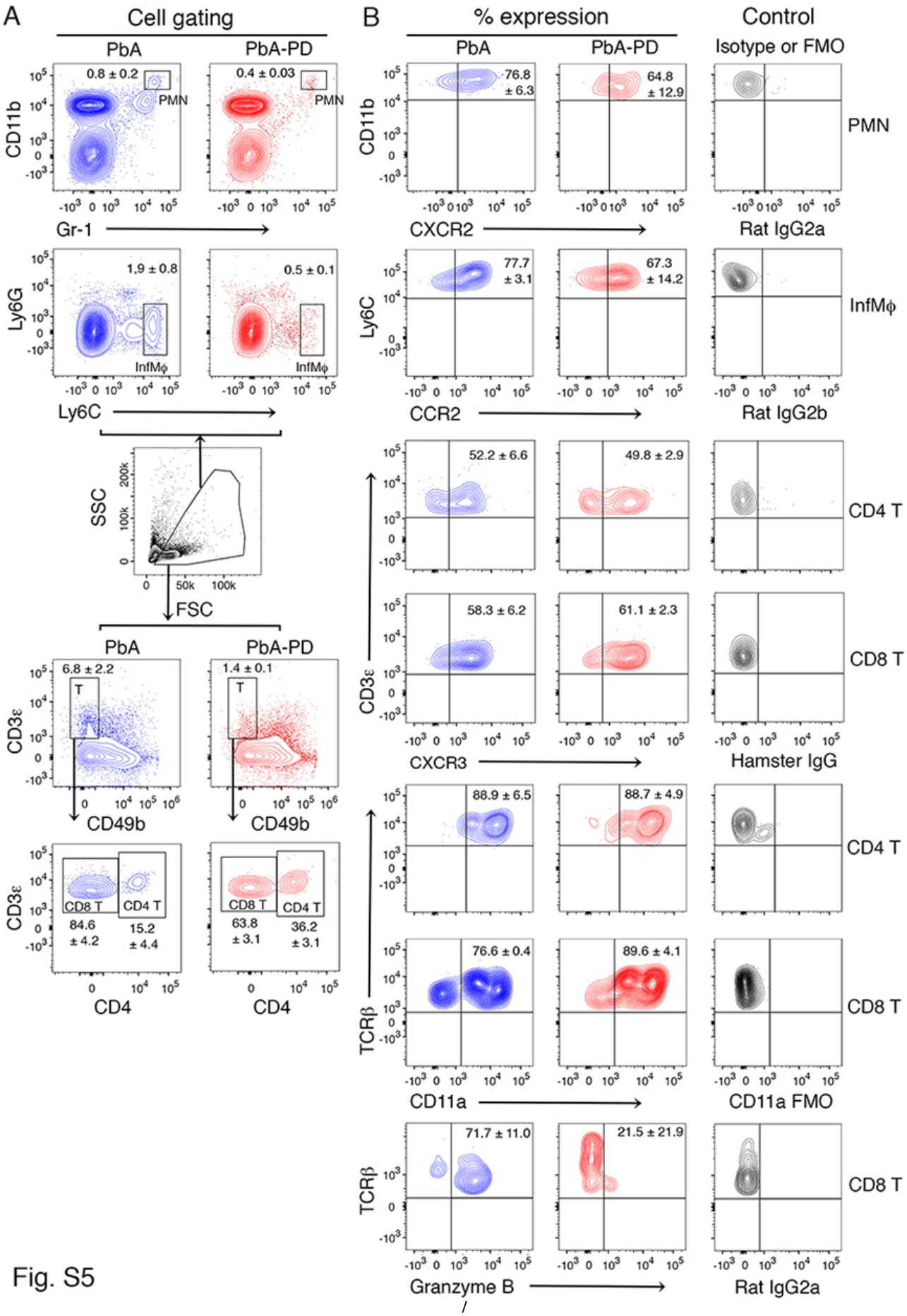
A
Cell gating
PbA
PbA-PD
0.8 ± 0.2
PMN
0.4 ± 0.03
PMN
CD11b
Gr-1
1.9 ± 0.8
InfMϕ
0.5 ± 0.1
InfMϕ
Ly6G
Ly6C
SSC
FSC
6.8 ± 2.2
T
1.4 ± 0.1
T
CD3ε
CD49b
CD8 T
CD4 T
84.6 ± 4.2
15.2 ± 4.4
63.8 ± 3.1
36.2 ± 3.1
CD4
B
% expression
Control
PbA
PbA-PD
Isotype or FMO
76.8 ± 6.3
64.8 ± 12.9
PMN
CXCR2
Rat IgG2a
77.7 ± 3.1
67.3 ± 14.2
InfMϕ
CCR2
Rat IgG2b
52.2 ± 6.6
49.8 ± 2.9
CD4 T
58.3 ± 6.2
61.1 ± 2.3
CD8 T
CXCR3
Hamster IgG
88.9 ± 6.5
88.7 ± 4.9
CD4 T
76.6 ± 0.4
89.6 ± 4.1
CD8 T
TCRβ
CD11a
CD11a FMO
71.7 ± 11.0
21.5 ± 21.9
CD8 T
Granzyme B
Rat IgG2a

Fig. S5

FIGURE S5. **Analysis immune cells infiltrated to the brains of ERK1/2 targeted PbA-infected mice**. Cells from the brain-homogenates of control and PD-treated mice PbA-infected mice at 6-day pi were stained with antibodies against the indicated surface markers, chemokine receptors, CD11a (LFA-1), and granzyme B. The cells were analyzed by flow cytometry; cells stained with isotype antibodies or FMO staining were used as controls. The results are presented in Fig. 11, *A*, *E* and *F*. The gating strategy (*panel A*) and percent chemokine receptor-, CD11a- and granzyme B-expressing cells infiltrated to the brain of untreated and PD-treated are shown (*panel B*).